Towards Optical Biopsies with an Integrated Fibered Confocal Fluorescence Microscope

Georges Le Goualher, Aymeric Perchant, Magalie Genet, Charlotte Cavé, Bertrand Viellerobe, Fredéric Berier, Benjamin Abrat, and Nicholas Ayache

Mauna Kea Technologies, 9, Rue d'Enghien,
75010 Paris, France
{georges,aymeric}@maunakeatech.com
http://www.maunakeatech.com

Abstract. This paper presents an integrated endoscope-compatible Fibered Confocal Fluorescence Microscope (FCFM) for medical imaging, the F-400. *In situ* high resolution images can be obtained thanks to a set of flexible miniaturized optical probes of 0.5 to 1.5 mm diameter that can be inserted through the working channel of an endoscope. We briefly present in this paper the FCFM system, with a particular focus on the image formation and the design of a dedicated image processing software allowing for drastically reduce the inherent artifacts occurring when imaging through an image bundle. The goal of the FCFM is to perform *optical biopsy* (i.e. *in vivo* and *in situ* observations of thin sections of biological tissues at the cellular level). As a first step towards this goal, we present here results of a clinical trial assessing the ability of the F-400 to perform rapid morphologic examination in the endoscopy room of medical specimens (polypectomy).

1 Introduction

In the very first step of epithelial cancer, abnormal cell proliferation first starts just above a specific tissue layer: the basal membrane, which is located at approximately 100 μm deep from the tissue surface for malpighian epithelium (cervix epithelium for example) and 300 μm for glandular epithelium (tissue that contains secretion glands: colon, pancreas, thyroid are examples of organs composed of glandular tissue). For such epithelial cancers (most cancers affecting solid organs), the medical procedure is to take a tissue sample (a biopsy) and to have it examined under the microscope of a pathologist. Most of these biopsy procedures are performed via endoscopy. However, an endoscope provides only a visualization of the surface of the tissue at a macroscopic level. It can neither see below the surface of the tissue nor provide a microscopic view of the tissue. Therefore, in a number of cases the best area to biopsy is difficult to assess. In order to improve the capability of an endoscope to perform early cancer detection, there is a need for an instrument that could provide a local sub-surfacic and high-resolution vision of the tissue, in other words to perform *optical biopsy*, *i.e.* non invasive optical sectioning within a thick transparent or translucent tissue with

high resolution. Several systems are today under study to reach the ultimate goal of performing *in vivo* and *in situ* optical biopsies. Let's first mention fluorescence spectroscopy where dysplasia and early carcinoma are detected based on the analysis of fluorescence spectra [1]. Drawback of fluorescence spectroscopy lies in the lack of morphological information (i.e. no cell architecture is available from this modality) and the important rate of false positives due to inflammatory processes. High magnification chromoscopic endoscopy (chromoendoscopy) has been introduced recently providing *in vivo* micro-architecture [2]. Magnification colonoscopic techniques when combined with colonic chromoscopy (dye spraying of the colon) permit *in vivo* assessments of lesions at a magnification and resolution similar to a stereoendoscope. In particular *in vivo* prediction of histological characteristics by crypt or pit pattern analysis can be performed using high magnification chromoendoscopy [3]. One drawback of this technique is that it cannot provide at the same time the macroscopic view (for global localization) and the zoomed image (for optical biopsy). We present here an integrated endoscope-compatible Fibered Confocal Fluorescence Microscope (FCFM) (we refer the reader to [4, 5] for other fibered systems). The confocal nature of the system makes it possible to observe sub-surfacic cellular structure (optical section parallel to the tissue surface at a depth from 0 to 100 μm), which is of particular interest for early detection of cancer. *In situ* imaging (typical lateral resolution of the images presented in this study are of 5 μm, axial resolution of 15 μm and field of view of 400x280 μm) can be obtained thanks to a set of flexible miniaturized optical probes of 0.5 to 1.5 mm diameter that can be inserted through the working channel of an endoscope. Note that, as the FCFM is used in conjunction with an endoscope, both macroscopic (endoscope image) as well as microscopic view (FCFM optical probe image) can be obtained at the same time, facilitating the selection of the area to be biopsied. As a first step towards the goal of *in vivo* and *in situ* optical biopsy, we present a related application which is the rapid morphologic examination in the endoscopy room of medical specimens, freshly excised, of colonoscopic polypectomy. First images acquired with the F-400 are presented showing that visual inspection of images may allow an expert to classify the pathology from the cell architecture.

2 Fibered confocal fluorescence microscopy system

A FCFM is based on the principle of confocal microscopy which is the ability to reject light from out-of-focus planes and provide a clear in-focus image of a thin section within the sample. This optical sectioning property is what makes the confocal microscope ideal for imaging thick biological samples. Schematically, the adaptation of a confocal microscope for *in situ* and *in vivo* imaging in the context of endoscopy can be viewed as replacing a microscope's objective by a probe of length and diameter compatible with the working channel of an endoscope in order to be able to perform *in situ* imaging. For such purpose, we used an image bundle is as the link between the scanning device and the microscope objective (see figure 1).

2.1 Image formation

A laser scanning unit, based on a laser at 488 nm, compatible with fluorescent dyes usable *in vivo* in clinical application, is scanned by two mirrors on the proximal surface of an optical image bundle. Horizontal line scanning is performed using a 4 kHz oscillating mirror while a galvanometric mirror performs frame scanning at 12 Hz. A custom synchronization hardware controls the mirrors and digitizes, synchronously with the scanning, the fluorescent signal using a mono-pixel photodetector. When organized according to the scanning, the output of the FCFM can be viewed as a raw image (see figure 3, left). Scanning amplitude and signal sampling frequency have been adjusted to perform a spatial over-sampling of the image bundle, this is clearly visible on the previous raw image where one can see individual fibers composing the bundle. Optical probes are composed of a connector, an image bundle and an optical head. The typical image bundle we use is composed of 30,000 optical fibers, with a fiber inter-core distance d_{ic} =3.3 µm, and a fiber core diameter of 1.9 µm.

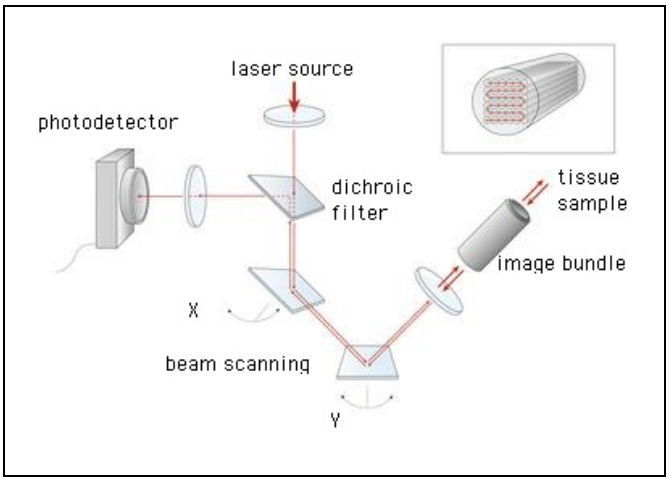

Fig. 1. Schematic principle of the FCFM

Critical elements in the image formation process lie in the correct spatial sampling of the image bundle by the scanning unit to avoid aliasing and the adjustment of the probe's optical head resolution (PSF) with this image bundle spatial sampling. In fact, when analyzing the probe's resolution with the sampling theory, we can consider that the optical resolution of the head corresponds to a low pass filter, and the image bundle to the sampling grid. The sampling Nyquist frequency of the image bundle is given by $2 * (1/d_{ic})$, which becomes $2 * (M/d_{ic})$ at the tissue focal plane, with M the magnification of the optical head (typical values of M goes from 1.0 to 2.5 depending on the probe's micro-optical head). The optical resolution of the head must therefore satisfy this frequency (as a rule

of thumb the FWHM of the optical head's PSF should be no larger that one-half of the minimal spatial period T_{min} of a sine wave that can be resolved given the Nyquist frequency ([6], page 373): $FWHM \approx 0.5 * T_{min} = 0.5 * (d_{ic}/M)$). The resulting lateral resolution of such a system is then: d_{ic}/M (*i.e.* the system has the ability to resolve a sine wave of period d_{ic}/M).

2.2 Image processing

To represent the raw data measured from a given optical fiber composing the image bundle, we propose the following model:

$$I = I_0 * \left(a * \tau_{inj} * \tau_{col} * \alpha_{fluo} + b * \tau_{inj} * \alpha_{autofluo}\right) \quad (1)$$

where a and b are constants[1], τ_{inj} and τ_{col} are injection rate, and collection rate of the fiber, $\alpha_{autofluo}$ is the intrinsic auto-fluorescence of the fiber, and α_{fluo} is the biological sample fluorescence we want to measure; I_0 is the intensity of the laser source. The task of the processing module is to restore the true physical measurement by removing the image bundle modulation (*i.e.* to estimate the biological sample fluorescence α_{fluo} given the raw data measured by each fiber I). Figure 2 presents the image processing sequence that was designed for this purpose.

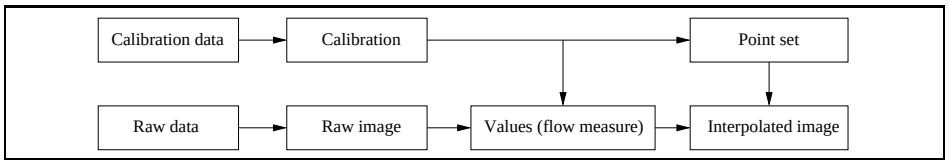

Fig. 2. Schematic principle of the image processing

Calibration – The image calibration process follows the top line of figure 2. As a preliminary step, we build a mapping between the FCFM raw image and the fibers composing the image bundle. Once the mapping between the raw data and each individual fiber is obtained, characteristics of each fiber are estimated. For this purpose, a non-fluorescent sample is imaged ($\alpha_{fluo} = 0$), followed by a sample of constant fluorescence ($\alpha_{fluo} = cst$). We note respectively I_b and I_s the associated measurements. The other output of the calibration is a point set representing the exact position of the fibers of the bundle.

Restoration – The image restoration process follows the bottom line of figure 2. The raw FCFM data is organized as a raw 2D image. Given the raw image to image bundle mapping, the fiber intensity I can be used in conjunction with the calibration data, to estimate the true physical measure (α_{fluo}), using the following equation:

[1] Note that more complicated intensity models can be proposed, i.e. where a and b are spatially variant, but we will not address them here

$$I_{restored} = \frac{I - I_b}{I_s - I_b} = K * \alpha_{fluo} \quad (K \; is \; a \; constant). \tag{2}$$

Reconstruction – At this step, we have a restored intensity: $I_{restored}$ for each fiber composing the image bundle. The final process is the interpolation of this point set into a numerical image on a square grid. The simplest method is the construction of a mosaic where all the pixels within the area of one fiber have a constant value. Other interpolation methods includes linear ($\mathcal{C}^0$ reconstruction), or cubic interpolation built from point set triangulation. For instance, the Clough-Tocher method allows a $\mathcal{C}^1$ reconstruction [7]. Considering that $\mathcal{C}^1$ reconstruction methods still present artifacts in particular for further image processing, $\mathcal{C}^2$ interpolations were also tested. Radial basis functions [8] allow such interpolation but at a high computational cost. We found that a B-spline iterative approximation, proposed by [9], was a good compromise between spatial continuity($\mathcal{C}^2$) and computational cost. In fact this method has a linear complexity in the number of points, and offers the possibility to control the reconstruction precision.

Results – A constant fluorescence solution (FITC) of controlled concentration to avoid detector saturation was imaged using the FCFM (see figure 3). If the true physical measurement was retrieved from the FCFM, the image should be constant (observed sample: $\alpha_{fluo} = cst$). The image on the left hand side of figure 3 represents the raw FCFM image. Note that individual fiber composing the image bundle are visible on this raw image, illustrating the correct spatial oversampling of the image bundle as well as the the interaction between each optical fiber and the laser spot transmission as a modulation of the true sample response. The image in the middle represents the reconstructed image using B-spline iterative approximation without any calibration step. The signal to noise ratio of this reconstructed image is 16 dB. Signal variations in this image are related to differences between individual fiber composing the image bundle. Given that the image bundle is made of fibers of different diameters and shapes, the transmission changes from one fiber to the other. The right image represents the reconstructed image using B-spline iterative approximation after restoration step was applied. The measured SNR in this image is now 32 dB. Residual noise on this image comes mainly from the electronic.

Finally, figure 4 is a comparison of a histologic section of a colonic tissue obtained by the pathologist with a restored and reconstructed image of a FCFM acquisition performed *in vivo* on a mouse [10]. Note that, on this normal tissue colonic crypts have the apearance of gun barrels. Typical size of such a colonic crypt on a mouse is 50 μm while it is 200 μm on humans.

2.3 Challenges

One of the main challenges for the design of the FCFM was to obtain a high laser coupling efficiency in a micron-sized fiber optic. For that purpose, a specific opto-mechanical connector has been designed to connect the probe to the scanning

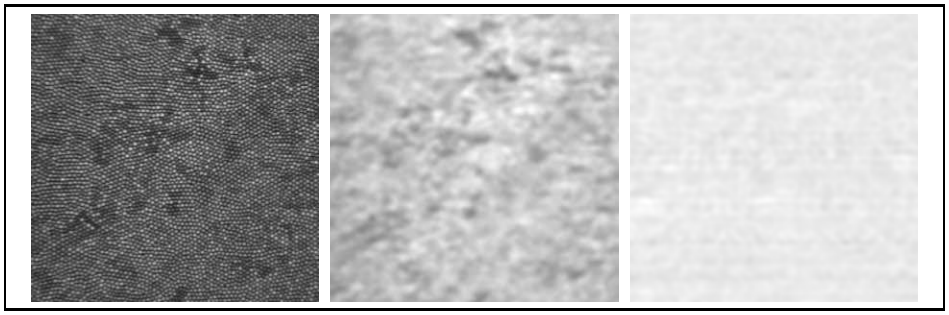

Fig. 3. From left to right: raw image of a constant signal, reconstruction without signal level calibration, and reconstruction using signal level calibration from equation 2. Uncalibrated image has a signal to noise ratio (SNR) of 16 dB, calibrated image of 32 dB.

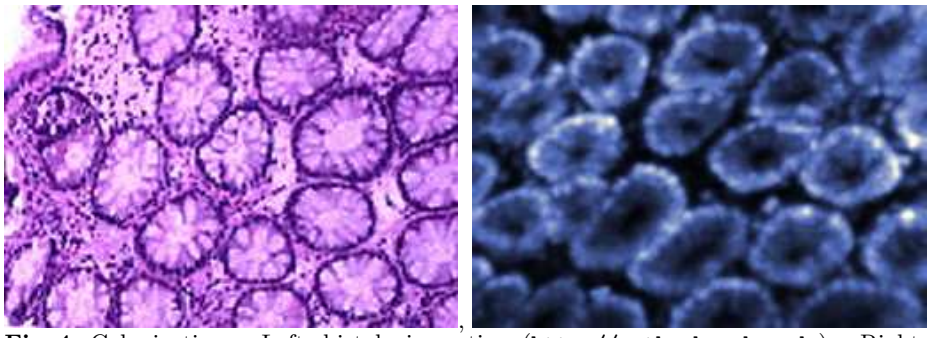

Fig. 4. Colonic tissue. Left: histologic section (`http://pathweb.uchc.edu`) ; Right: FCFM processed image (restored and reconstructed). FOV: 400x280 μm (image courtesy of Igor Charvet, CMU, Geneva, Switzerland)

unit. The connector gives a high repeatability in the focus position, as well as the optimal injection along the whole image field. Finally, the optical wave front error of the scanning beam has been optimized to ensure that only one fiber is injected at a time. When dealing with signal processing, the challenge resides here in the correct modeling of the data transmission and acquisition process has well and the real-time constraint on image processing (12 Hz).

3 Optical biopsies of freshly excised colonoscopic polypectomy

In this section, we present the first images obtained by the FCFM on freshly human excised colonoscopic polypectomy. The protocol was the following: during a colonoscopy, polyps on the wall of the colon were localized using the macroscopic view provided by the endoscope. Before resection of a polyp, a catheter containing a vital dye commonly used in chromoendoscopy (cresyl violet) was

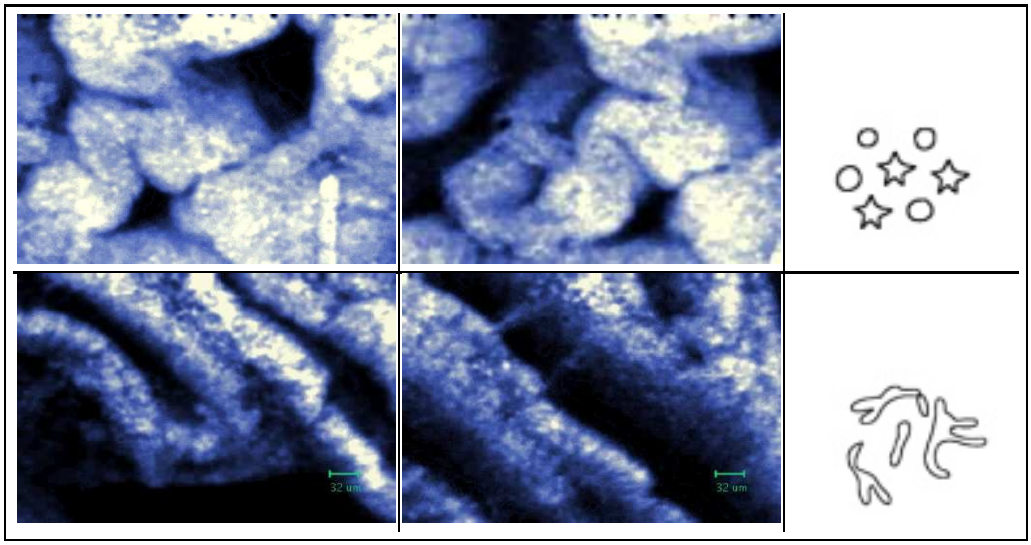

Fig. 5. Freshly excised specimens observed using the FCFM. Lateral resolution is about 5 μm, axial resolution is about 15 μm, Field of view is 400x280 μm. Top: hyperplastic polyp. Bottom: tubulo-villous adenoma with low grade dysplasia. Right column: schematic representation taken from the classification of Kudo ([3])

inserted within the working channel of the endoscope. Cresyl violet offers contrast by accentuating the morphological landscape of tissues and is commonly used for chromoendoscopy of the colon. A very important property of cresyl violet is that, eventhough it is not considered to be a fluorescent dye but a vital dye (therefore not toxic for cells) it becomes fluorescent when excited at 488 nm allowing imaging to be performed by the FCFM. In fact, cresyl violet was successfully tested as a fluorophore for histopathology with confocal laser scanning microscope (CLSM) [11]. Once the polyp is resected, the FCFM is used to image the freshly excised sample. Figure 5 represents a sample of acquired images. Note that the micro-architecture of the tissue sample is clearly visible on these images. Using the Kudo "Pit Pattern" classification ([3]), visual inspection of the two images in the top raw on figure 5 suggest hyperplastic polyps (*type II* in the Kudo nomenclature) since the shape and size of the colonic crypts are similar to those associated with the corresponding Kudo diagram (right image). Note in particular *star-like* shape of the colonic cript in the inferior part of the image. Using the same methodology, sizes and shapes of colonic crypts as observed on the bottom raw, suggest tubulo-villous adenoma with low grade dysplasia (*type IIIL* in the Kudo classification).These assumptions were confirmed by a pathologist after histology.

4 Conclusion

An integrated fibered confocal system for *in vivo* and *in situ* fluorescence imaging has been presented. As a first step towards *in vivo* and *in situ* optical biopsy, we have presented here first images obtained on freshly excised surgical specimens. On reconstructed images, micro-architecture is clearly visible (colonic crypt organization) suggesting that these images could be used by an expert to detect and classify underlying pathologies. A clinical trial is currently under way to study the capability of the FCFM to provide biopsy guidance which will be of particular interest for the analysis of flat adenomas (*i.e.* adenomas very difficult to localize at the macroscopic scale) and assessment of tumor margins. Future works include the study of micro-optic designs in order to get an improved cellular resolution.

References

1. Bourg-Heckly, G., Blais, J., Padila, J.J., Bourdon, O., Etienne, J., Guillemin, F., Lafay, L.: Endoscopic ultraviolet-induced autofluorescence spectroscopy of the esophagus : tissue characterization and potential for early cancer diagnosis. Endocopy **32** (2000) 756–765
2. Jaramillo, E., Watanabe, M., et al., P.S.: Flat neoplastic lesions of the colon and rectum detected by high-resolution video endoscopy and chromoscopy. Gastrointestinal Endoscopy **42** (1995) 114–122
3. Kudo, S., Rubio, C., Teixeira, C., Kashida, H., Kogure, E.: Pit pattern in colorectal neoplasia: endoscopic magnifying view. Endoscopy **33** (2001) 367–373
4. Sabharwal, Y., Rouse, A., Donaldson, L., Hopkins, M., Gmitro, A.: Slit-canning confocal microendoscope for high-resolution in vivo imaging. Applied optics **38** (1999) 7133–7144 classeur confocal fibr - 049.
5. Sung, K., Liang, C., Descour, M., Collier, T., Follen, M., Richard-kortum, R.: Fiber optic reflectance for in vivo imaging of human tissues. IEEE Transactions on biomedical engineering **49** (2002) 1168–1172
6. Castleman, K.R.: Digital Image Processing. Prentice Hall (1996) ISBN 0-13-211467-4.
7. Amidror, I.: Scattered data interpolation methods for electronic imaging systems: a survey. Journal of Electronic Imaging **11** (2002) 157–176
8. Carr, J.C., Beatson, R.K., Cherrie, J., Mitchell, T.J., Fright, W.R., McCallum, B.C., Evans, T.R.: Reconstruction and representation of 3D objects with radial basis functions. In: ACM SIGGRAPH, Los Angeles (2001) 67–76
9. Lee, S., Wolberg, G., Shin, S.Y.: Scattered data interpolation with multilevel B-splines. IEEE Transactions on Visualization and Computer Graphics **3** (1997) 228–244
10. Perchant, A., Le Goualher, G., Genet, M., Viellerobe, B., Berier, F.: An integrated device for *in vivo* and *in situ* fluorescence confocal microscopy for endoscopic images in small animals. In: IEEE International Symposium on Biomedical Imaging: From Nano to Macro. (2004) to appear.
11. Meining, G.M.: Cresyl violet as a fluorophore in confocal laser scanning microscopy for future in vivo histopathology. Endoscopy **35** (2003) 585–589